An Omnidirectional Vision-Based Moving Obstacle Detection in Mobile Robot

Jongcheol Kim and Yasuo Suga*

Abstract: This paper presents a new moving obstacle detection method using an optical flow in mobile robot with an omnidirectional camera. Because an omnidirectional camera consists of a nonlinear mirror and CCD camera, the optical flow pattern in omnidirectional image is different from the pattern in perspective camera. The geometry characteristic of an omnidirectional camera has influence on the optical flow in omnidirectional image. When a mobile robot with an omnidirectional camera moves, the optical flow is not only theoretically calculated in omnidirectional image, but also investigated in omnidirectional and panoramic images. In this paper, the panoramic image is generalized from an omnidirectional image using the geometry of an omnidirectional camera. In particular, Focus of expansion (FOE) and focus of contraction (FOC) vectors are defined from the estimated optical flow in omnidirectional and panoramic images. FOE and FOC vectors are used as reference vectors for the relative evaluation of optical flow. The moving obstacle is turned out through the relative evaluation of optical flows. The proposed algorithm is tested in four motions of a mobile robot including straight forward, left turn, right turn and rotation. The effectiveness of the proposed method is shown by the experimental results.

Keywords: FOE and FOC vectors, moving obstacle detection, omnidirectional camera, optical flow.

1. INTRODUCTION

It is indispensable to detect the obstacles and free space for locomotion of the mobile robot in real-world environment. Recently, vision-based environment detection methods have been actively developed in robot vision [1-3]. The vision system can provide not only a huge amount of information but also color information in the populated environment. Currently, because the omnidirectional vision system [4,5] supplies a wide view of 360 degrees, they have been popularly used in many applications such as the motion estimation [6-10], environment recognition [11,12], localization [13,14], and navigation [15-17] of a mobile robot.

In the past few years, moving obstacle detection and motion estimation methods using the optical flow for a mobile robot with a perspective camera [18-25] have been actively developed. In [18], a qualitative obstacle detection method was proposed using the directional divergence of the motion field. In [22], the optical flow pattern was investigated in perspective camera and this pattern was used for moving object detection. In [25], real-time moving object detection method was presented during translational robot motion.

The optical flow pattern in a perspective camera [22] is different from the pattern in an omnidirectional camera because of the distortion of an omnidirectional mirror. Some researches have been also developed for ego-motion estimation and/or navigation of a mobile robot with an omnidirectional image [6-9,11,26,27]. In [6], ego-motion algorithm was presented using an omnidirectional camera. The optical flow was mapped to a sphere for estimating ego-motion using the Jacobian of the transformation between the projection model of the camera and spherical projection. In [27], the unknown obstacle detection method was presented using a HyperOmni vision. After features had been corresponded to consecutive perspective transformed images of omnidirectional images, unmatched features

Manuscript received February 24, 2006; revised March 6, 2007; accepted September 19, 2007. Recommended by Editorial Board member Hoon Kang under the direction of Editor Jae-Bok Song. This work was supported in part by Grant in Aid for the 21st century center of excellence for "System Design: Paradigm Shift from Intelligence to Life" from Ministry of Education, Culture, Sport and Technology in Japan.

Jongcheol Kim is with the Robot Business Department, KT, 17 Woomyeon-dong, Seocho-gu, Seoul 135-792, Korea (e-mail: jckim07@kt.co.kr).

Yasuo Suga is with the Department of Mechanical Engineering, Faculty of Science and Technology, Keio University, 3-14-1 Hiyoshi, Kouhoku-ku, Yokohama, 223-8522, Japan (e-mail: suga@mech.keio.ac.jp).

* Corresponding author.

were recognized as obstacles. In [7], the infinitesimal motion estimation method was proposed using an optical flow equation derived directly from a central panoramic camera. In [8], the Jacobian matrix of a general projection model was introduced for ego-motion estimation from the motion field on sphere. A general projection model represents all single projection center camera. In [11], dynamic event detection and tracking methods were proposed using ego-motion compensation and flat-plan transformation. The optical flow was applied for estimating the motion parameters of an omnidirectional camera. In [26], Focus-Of-Expansion (FOE) and Focus-Of-Contraction (FOC) points in omnidirectional image were used in order to estimate the independent object movement. Although FOE and FOC positions in omnidirectional image were utilized for robot navigation [26], FOE and FOC positions were not theoretically analyzed and optical flow pattern arising from mirror distortion was not investigated in detail. In this paper, FOE and FOC points are mathematically derived as well as the pattern of optical flow in omnidirectional and panoramic images is precisely analyzed for detecting the moving object. In particular, the derived FOE and FOC points depend on not image pixel coordinates but the linear and angular velocities of a mobile robot.

We propose a new moving object detection method using optical flow in an omnidirectional camera mounted on a mobile robot. We focus on the optical flow in omnidirectional camera. First of all, an omnidirectional image is converted into a human-friendly panoramic image. The moving object is detected in panoramic image. In omnidirectional image, the length of optical flow becomes large according as the radial distance goes away from the center point. Otherwise, in panoramic image, the length of optical flow becomes is not affected from radial distance of omnidirectional image. Next, optical flow pattern is analyzed in omnidirectional and panoramic images. When a mobile robot has translation motion, FOE and FOC points of optical flow exist. In particular, Focus of expansion (FOE) and focus of contraction (FOC) vectors are defined from the estimated optical flow in omnidirectional and panoramic images. FOE and FOC vectors are used as reference vectors for the relative evaluation of optical flow. The moving obstacle is turned out through the relative evaluation of optical flows. However, if the motion of a mobile robot is only rotation, FOE and FOC points do not exist. In this case, the special characteristic of optical flow is utilized. The proposed algorithm is tested in four motions of a mobile robot including straight forward, left turn, right turn and rotation.

The rest of this paper is organized as follows. The geometry model of an omnidirectional camera and the panoramic expansion of omnidirectional image are described in Section 2. In Section 3, the optical flow is analyzed in omnidirectional image. FOE and FOC vectors are also defined. The moving obstacle detection algorithm is described in Section 4. Experiment results and discussion of the proposed method are illustrated in Section 5. Conclusion is given in Section 6.

2. OMNIDIRECTIONAL VISION SYSTEM

2.1. Geometry model of an omnidirectional camera

The omnidirectional camera is mounted on a mobile robot. An omnidirectional vision consists of a CCD camera and a curved mirror. A hyperbolic mirror is used as a curved mirror in this paper. The geometry of the hyperbolic omnidirectional camera is shown in Fig. 1. An omnidirectional image on image plane x-y is generated through the following process. Firstly, a light ray goes ahead to mirror focal point O_m from the object point $P(X,Y,Z)$ in the field of 360 degrees around the Z axis of omnidirectional image. Next, a light ray is reflected toward a camera lens focal point O_c as shown in Fig. 1.

The hyperboloidal equation of the mirror is presented as:

$$\frac{X^2+Y^2}{a^2}-\frac{(Z+c)^2}{b^2}=-1, \qquad c=\sqrt{a^2+b^2}, \tag{1}$$

where a and b are parameters of the hyperboloidal mirror shape.

The relationship between an image position $p(x,y)$ and a real-world 3D position $P(X,Y,Z)$ is presented as follows:

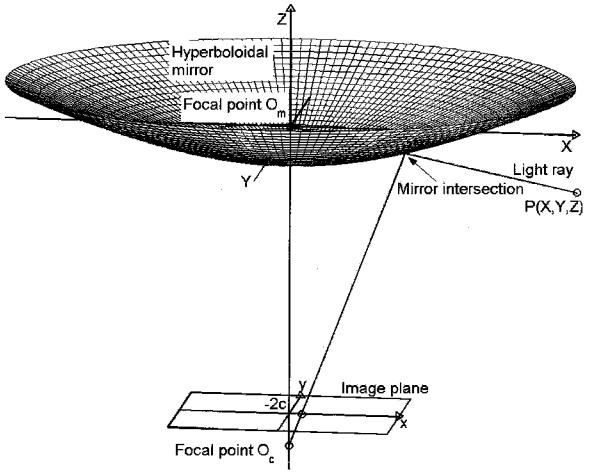

Fig. 1. Geometry of hyperboloidal projection.

$$\begin{bmatrix} x \\ y \end{bmatrix} = \frac{f(b^2 - c^2)}{(b^2 + c^2)Z - 2bc\sqrt{X^2 + Y^2 + Z^2}} \begin{bmatrix} X \\ Y \end{bmatrix}, \quad (2)$$

where f is the focal length of a camera.

2.2. Panoramic expansion of omnidirectional image

An omnidirectional image is converted into a panoramic image. A virtual cylindrical image plane is firstly set around an omnidirectional camera as shown in Fig. 2. Each point $P(X,Y,Z)$ on cylindrical image plane is projected using (2) onto an omnidirectional image. The intensity value of pixel in panoramic image is determined using a linear interpolation method in omnidirectional image. Fig. 3(a) shows the original omnidirectional image of cylindrical square pattern. Fig. 3(b) shows the expanded panoramic image from the omnidirectional image in Fig. 3(a) using only the transformation of polar coordinates in omnidirectional image into Cartesian coordinates. Fig. 3(c) shows the expanded panoramic image from the omnidirectional image in Fig. 3(a) using (2). In this paper, the panoramic image is utilized using (2) as shown in Fig. 3(c).

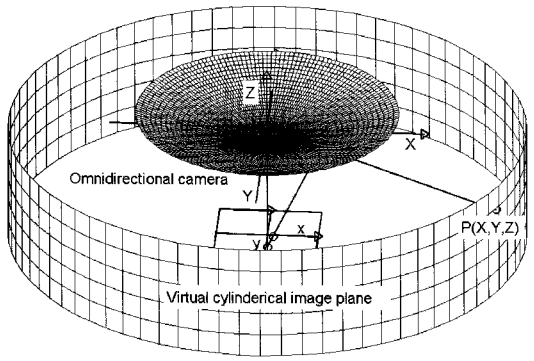

Fig. 2. Virtual cylindrical image plane.

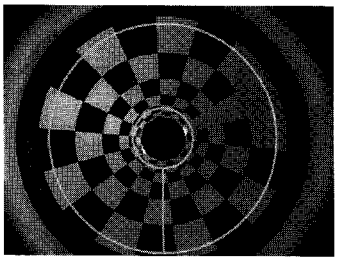

(a) Omnidirectional image

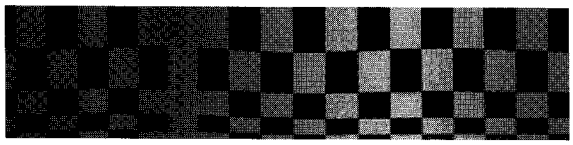

(b) Panoramic image using the transformation of polar coordinates on omnidirectional image into Cartesian coordinates.

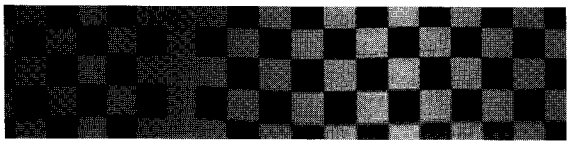

(c) Panoramic image using the transformation of (2)

Fig. 3. Expanded panoramic images from the omnidirectional image.

3. OPTICAL FLOW ANALYSIS AND FOE AND FOC VECTORS

In this section, the optical flow in omnidirectional and panoramic images is investigated. The optical flow relates to the velocities of the mobile robot with an omnidirectional camera. FOE and FOC vectors are defined from the estimated optical flow.

3.1. Optical flow in omnidirectional image

The hyper-catadioptric projection equation [7] from (2) can be written as follows:

$$\lambda \mathbf{x} = FP, \quad (3)$$

where $\mathbf{x} = (x, y, 0)^T$, $F = diag(1,1,0) \in \mathbb{R}^{3\times 3}$, $P = (X, Y, Z)^T$ and

$$\lambda = \frac{(b^2 + c^2)Z - 2bc\sqrt{X^2 + Y^2 + Z^2}}{f(b^2 - c^2)}.$$

The rigid motion of a scene point P which is related to a camera motion can be described using a linear velocity $V = (V_x, V_y, V_z)^T$ and an angular velocity $\Omega = (\Omega_x, \Omega_y, \Omega_z)^T$. The instantaneous velocity [6] of a scene point P in camera frame is evolved as follows:

$$\dot{P} = -V - \Omega \times P. \quad (4)$$

The differentiating equation of (3) with respect to time is a $\dot{\lambda}\mathbf{x} + \lambda\dot{\mathbf{x}} = F\dot{P}$.

Consequently, optical flow $\dot{\mathbf{x}} = (\dot{x}, \dot{y})^T$ is obtained as follows:

$$\begin{bmatrix} \dot{x} \\ \dot{y} \end{bmatrix} = \frac{1}{\lambda} \begin{bmatrix} -1 + \varepsilon\lambda x^2 & \varepsilon\lambda xy & \frac{\alpha}{\beta}x + \varepsilon xZ \\ \varepsilon\lambda xy & -1 + \varepsilon\lambda y^2 & \frac{\alpha}{\beta}y + \varepsilon yZ \end{bmatrix} V + \begin{bmatrix} \frac{\alpha}{\beta}xy & -\frac{Z}{\lambda} - \frac{\alpha}{\beta}x^2 & y \\ \frac{Z}{\lambda} + \frac{\alpha}{\beta}y^2 & -\frac{\alpha}{\beta}xy & -x \end{bmatrix} \Omega, \quad (5)$$

where $\alpha = b^2 + c^2$, $\beta = f(b^2 - c^2)$, $\varepsilon = -2bc/(\beta \mid P \mid)$,

and $|P|=\sqrt{X^2+Y^2+Z^2}$.

3.2. Definition of FOE and FOC vectors

Since a mobile robot moves only on $X-Y$ plane in this paper, the linear velocity is $V=(V_x,V_y,0)^T$ and the angular velocity is $\Omega=(0,0,\Omega_z)^T$. The hyper-catadioptric optical flow of (5) is rewritten as:

$$\begin{bmatrix}\dot{x}\\ \dot{y}\end{bmatrix}=\frac{1}{\lambda}\begin{bmatrix}-1+\varepsilon\lambda x^2 & \varepsilon\lambda xy\\ \varepsilon\lambda xy & -1+\varepsilon\lambda y^2\end{bmatrix}\begin{bmatrix}V_x\\ V_y\end{bmatrix}+\begin{bmatrix}y\\ -x\end{bmatrix}\Omega_z. \quad (6)$$

If a mobile robot has only rotation motion, optical flow $(\dot{x},\dot{y})^T$ is presented as follows:

$$\begin{bmatrix}\dot{x}\\ \dot{y}\end{bmatrix}=\begin{bmatrix}y\\ -x\end{bmatrix}\Omega_z. \quad (7)$$

On the contrary, if a mobile robot has only translation motion, optical flow $(\dot{x},\dot{y})^T$ is presented as follows:

$$\begin{bmatrix}\dot{x}\\ \dot{y}\end{bmatrix}=\frac{1}{\lambda}\begin{bmatrix}-1+\varepsilon\lambda x^2 & \varepsilon\lambda xy\\ \varepsilon\lambda xy & -1+\varepsilon\lambda y^2\end{bmatrix}\begin{bmatrix}V_x\\ V_y\end{bmatrix}. \quad (8)$$

In case of translation motion, there are two points $(x,y)^T$ where optical flow $(\dot{x},\dot{y})^T$ of (8) is zero. Then, two points $(x,y)^T$ are calculated as follows:

$$\begin{bmatrix}x\\ y\end{bmatrix}=\pm\frac{1}{\sqrt{\varepsilon\lambda(V_x^2+V_y^2)}}\begin{bmatrix}|V_x|\\ V_xV_y/|V_x|\end{bmatrix},\text{if } |V_x|\neq 0 \quad (9)$$

or

$$\begin{bmatrix}x\\ y\end{bmatrix}=\pm\frac{1}{\sqrt{\varepsilon\lambda(V_x^2+V_y^2)}}\begin{bmatrix}V_xV_y/|V_y|\\ |V_y|\end{bmatrix},\text{if } |V_y|\neq 0. \quad (10)$$

These two points $(x,y)^T$ become candidates for Focus-of-Expansion (FOE) and Focus-of-Contraction (FOC) points. In omnidirectional and panoramic images, the optical flow seems to be emerging on FOE point, on the contrary, the optical flow seems to be vanishing on FOC point. In this paper, FOE and FOC vectors are defined as vectors from center point to FOE and FOC points in omnidirectional image, respectively. In the panoramic image, they are defined as vertical vectors from bottom to top.

Fig. 4 shows optical flows, FOE and FOC vectors in omnidirectional and panoramic images. FOE and FOC vectors are illustrated as (1) and (2) arrows respectively. If a mobile robot has the motion of straight forward, in omnidirectional image FOE and FOC vectors are situated at opposite direction as shown in Fig. 4(a). The shape of optical flow is symmetric in according to the line of FOE and FOC vectors. In panoramic image as shown in Fig. 4(a), a FOE vector are situated in the middle part of panoramic image and a FOC vector set in the edge of panoramic image. However, FOE and FOC vectors do not exist in only rotation. When a mobile robot has the motion of right turn, FOE and FOC vectors are described on left side of omnidirectional image. Also, they are described on right side of omnidirectional image on the motion of left turn. These optical flow pattern is characterized as shown in Fig. 4(c) and (d).

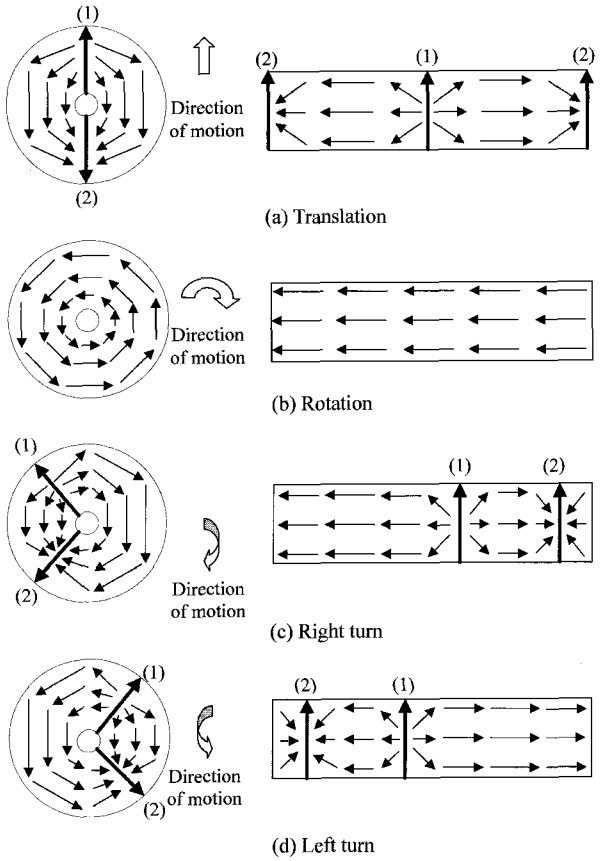

Fig. 4. Optical flows, FOE (1) and FOC (2) vectors in omnidirectional and panoramic images.

In particular, the length optical flow becomes large in the middle of between FOE and FOC vector. However, it becomes small in the neighborhood of between FOE and FOC vector. These pattern is used for determining the relative evaluation of optical flows in Section 4.

In Fig. 5, FOE (1) and FOC (2) vectors estimated experimentally in omnidirectional image are shown. Fig. 6 also shows the estimated FOE (1) and FOC (2) vectors in panoramic image. When a mobile robot has four movements including straight forward, rotation, right turn and left turn, results of estimated optical flows and FOE and FOC vectors in Figs. 5 and 6 are similar to the characteristics of those shown in Fig. 4.

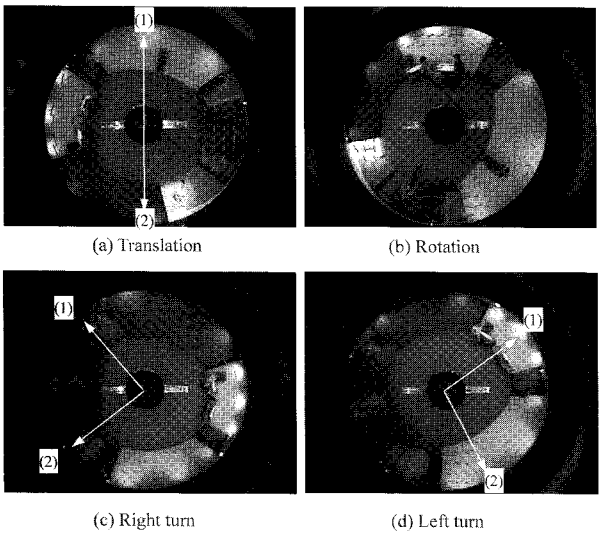

Fig. 5. Estimated FOE (1) and FOC (2) vectors in omnidirectional image.

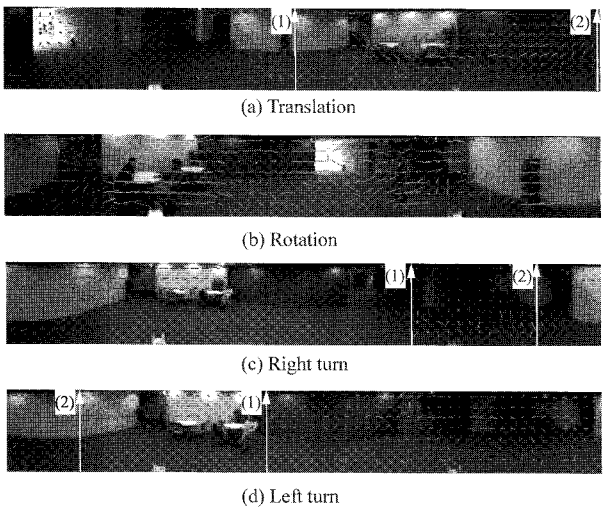

Fig. 6. Estimated FOE (1) and FOC (2) vectors in panoramic image.

4. MOVING OBJECT DETECTION ALGORITHM

In this section, the moving objects detection algorithm in panoramic image is described. The algorithm flowchart for detecting moving objects is shown in Fig. 7. The moving objects detection algorithm is summarized by the following procedure.

Step 1: The omnidirectional image captured from CCD camera is monochromized to gray image.

Step 2: The omnidirectional image is expanded into panoramic image using (2). The intensity of each pixel in panoramic image is determined using the linear interpolation method.

Step 3: The optical flow in panoramic image is calculated. The optical flow is computed using the well known spatial local optimization proposed by

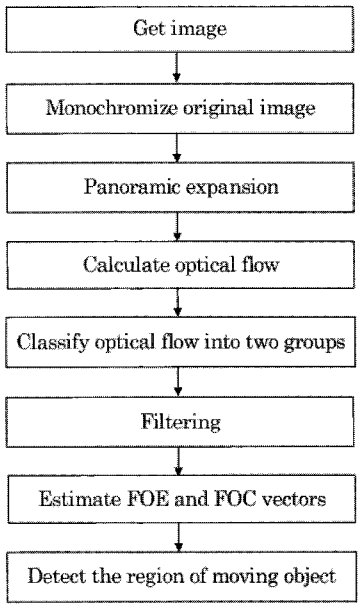

Fig. 7. Flowchart for detecting moving object.

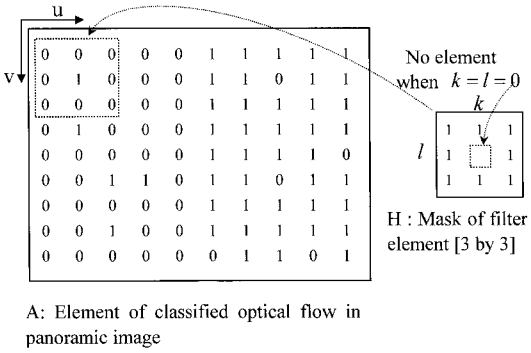

Fig. 8. Filtering.

Lucas and Kanade method [28] for fast processing time. The spatial local region is [10×10] pixels.

Step 4: The noise of the estimated optical flow is eliminated using filtering. The vibration of a mobile robot causes the noise of optical flow. Before the filtering, estimated optical flows are classified into two groups in according to the direction of optical flow vector. The direction of optical flow vector is determined from the size of internal angle between an optical flow vector and the u-axis of Cartesian coordinates; u and v axis in panoramic image. If the size of the absolute value of internal angle is larger than 90°, the direction of optical flow vector is assigned to zero. If the size of the absolute value of internal angle is smaller than 90°, the direction of optical flow vector is assigned to one. As one example, the classified element (0 and 1) image is shown in Fig. 8.

For filtering, suppose that the element image of the classified optical flow and the mask of filter element are $A(i, j)$ and $H(i, j)$ respectively, the following convolution is calculated,

Table 1. Output of the filter.

#1	#0	$f(i,j)$	Output of filter $A(i,j)$
8	0	8	1
7	1	7	1
6	2	6	1
5	3	5	$A(i,j)$
4	4	4	$A(i,j)$
3	5	3	$A(i,j)$
2	6	2	0
1	7	1	0
0	8	0	0

$$f(i,j)=\sum_{k=-1}^{1}\sum_{l=-1}^{1}A(i+k,j+l)H(k,l), \qquad (11)$$

where $k=l\neq 0$ and (i,j) is the coordinates of optical flow. The filtering is accomplished as follows:

$$\begin{cases} A(i,j)=1, & \text{if } f(i,j)>=6, \\ A(i,j)=A(i,j), & \text{if } 2<f(i,j)<6, \\ A(i,j)=0, & \text{if } f(i,j)<=2. \end{cases}$$

Table 1 describes output of the filter. #1 and #0 are the numbers of elements 1 and 0 in $[3\times 3]$ matrix of $A(i,j)$ around (i,j). The maximum and minimum of $f(i,j)$ are 8 and 0. Filter thresholds are set as 6 and 2 on the basis of the truth 66.7% of same elements 1 or 0 around (i,j). In the middle part $\{3,4,5\}$, the filter output keeps up the current element $A(i,j)$.

Step 5: FOE and FOC vectors are estimated from the filtered optical flow.

FOE and FOC points can be ideally obtained from positions where the size of the optical flows is zero. However, it is difficult to find FOE and FOC points directly as shown in (6). In this paper, FOE and FOC vectors are found using the histogram of angles of optical flow. To begin with, the angle of optical flow is defined as the angle of start point of optical flow an according to the u-axis in panoramic image. The histogram is investigated in the selected right region from two groups classified in Step 4.

Fig. 9(a) and (b) show the angles of optical flow defined in omnidirectional and panoramic images, respectively. The maximum (h_{max}) and minimum (h_{min}) of histogram angles become the candidates of angles of FOE and FOC vectors. The threshold is used to find proper maximum and minimum of histogram angles. When the mobile robot moves forward, the angles of FOE and FOC vectors are determined as follows:

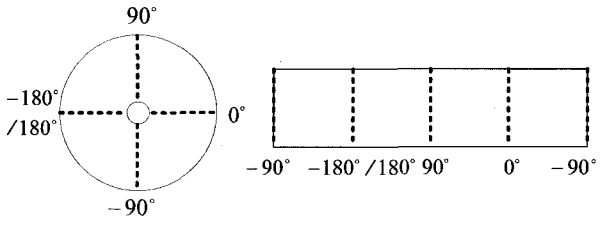

(a) Omnidirectional image (b) Panoramic image

Fig. 9. Angle of optical flow.

(a) Expanded panoramic image

(b) Classified optical flow in two groups

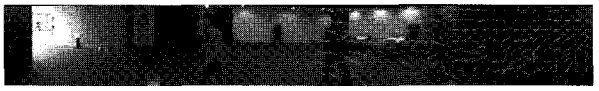

(c) Selected right region group

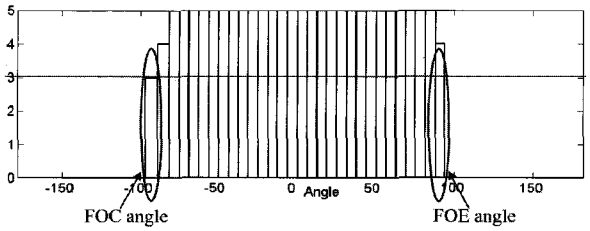

(d) Angles of FOE and FOC vectors extracted from histogram of optical flow in (c)

(e) Extracted FOE (1) and FOC (2) vectors

Fig. 10. Extraction of FOE and FOC vectors.

$$\begin{cases} \text{if } h_{max}+h_{min}>-180, \\ \quad \text{Angles of FOE vector} = h_{max}, \\ \quad \text{Angles of FOC vector} = h_{min} \\ \text{otherwise} \\ \quad \text{Angles of FOE vector} = h_{min}, \\ \quad \text{Angles of FOC vector} = h_{max}. \end{cases}$$

Fig. 10 shows the extraction process of FOE and FOC vectors when a mobile robot moves to straight forward. The classified two optical flow groups is illustrated in Fig. 10(b). The selected right region from two optical flow groups is shown in Fig. 10(c).

The histogram of angles of optical flow is investigated in selected right region. In Fig. 10(d), the interval of histogram angle axis is 6.27 degrees. The threshold is set experientially as 3 in order to find proper maximum and minimum of histogram angles. The maximum and minimum of the histogram selected from threshold of Fig. 10(d) are angles of FOE (1) and FOC (2) vectors, respectively. Angles of FOE (1) and FOC (2) vectors illustrated in Fig. 10(e) are 92.02 and -84.54 degrees.

Step 6: Moving objects are detected using the evaluation value.

The optical flow of the moving object is turned out through the relative evaluation of optical flows. FOE and FOC vectors are used as reference vectors for the relative evaluation of optical flows. As invested in Section 3, the length of optical flow becomes small in the neighborhood of FOE and FOC vectors, but large in the middle of between FOE and FOC vectors. FOE and FOC vectors exist on translation motion of mobile robot, but they do not exist on only rotation motion. In rotation case, the length and direction of optical flow are investigated. These characteristics supply the clue for extracting moving objects from optical flows.

Two evaluation values are proposed for extracting moving objects in cases of translation and rotation. In case of translation including straight, left turn and right turn motions, let optical flow vector be $\vec{v}_{ij} = \vec{v}_{x_{ij}} + \vec{v}_{y_{ij}}$, for $i = 1$ and 2, which i is the classified groups of optical flows and $j = 1,...,M$ or N, M and N are the number of optical flows when $i = 1$ and $i = 2$, respectively. The evaluation value $E_{t_{ij}}$ is defined as follows:

$$E_{t_{ij}} = \frac{L_{\vec{v}_{ij}}}{\|\mathbf{L}_{\vec{v}}\|} \frac{L_{\vec{v}_{x_{ij}}}}{\|\mathbf{L}_{\vec{v}_x}\|}(-0.5sin(\theta_{ij}) + 1), \quad (12)$$

where $L_{\vec{v}_{ij}}$ and $L_{\vec{v}_{x_{ij}}}$ are the length of $\vec{v}_{ij}$ and $\vec{v}_{x_{ij}}$, respectively, $\mathbf{L}_{\vec{v}} = [L_{\vec{v}_{11}}, L_{\vec{v}_{12}}, ..., L_{\vec{v}_{1M}}, L_{\vec{v}_{21}}, L_{\vec{v}_{22}}, ..., L_{\vec{v}_{2N}}]$, and $\mathbf{L}_{\vec{v}_x} = [L_{\vec{v}_{x11}}, L_{\vec{v}_{x12}}, ..., L_{\vec{v}_{x1M}}, L_{\vec{v}_{x21}}, L_{\vec{v}_{x22}}, ..., L_{\vec{v}_{x2M}}]$, $\|\mathbf{L}_{\vec{v}}\|$ and $\|\mathbf{L}_{\vec{v}_x}\|$ are the norms of $\mathbf{L}_{\vec{v}}$ and $\mathbf{L}_{\vec{v}_x}$, respectively. $L_{\vec{v}_{ij}}/\|\mathbf{L}_{\vec{v}}\|$ and $L_{\vec{v}_{x_{ij}}}/\|\mathbf{L}_{\vec{v}_x}\|$ mean the normalized quantities of $\mathbf{L}_{\vec{v}}$ and $\mathbf{L}_{\vec{v}_x}$. $\theta_{ij} = 180\alpha_{ij}/\beta_i$. Values $\vec{v}_{ij}$, $\vec{v}_{x_{ij}}$, $\vec{v}_{y_{ij}}$, α_{ij} and β_i are shown in Fig. 11. As shown in Fig. 11, $\beta_1 + \beta_2 = 360$, $0° < T < 360°$, $0 \le \alpha_{1j} \le \beta_1$ and $0 \le \alpha_{2j} \le \beta_2$.

Fig. 12 shows the characteristic of the evaluation parameter $E_{t_{ij}}$. Under condition without moving obstacles, $E_{t_{ij}}$ is investigated into three motions of a

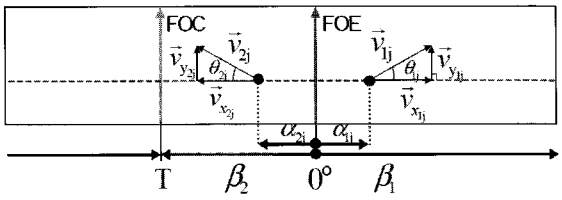

Fig. 11. Definition of evaluation values.

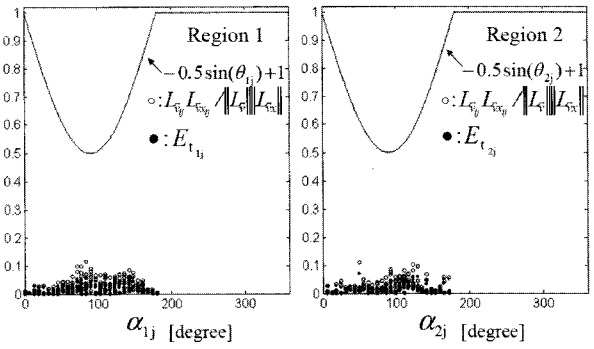

(a) Straight forward.

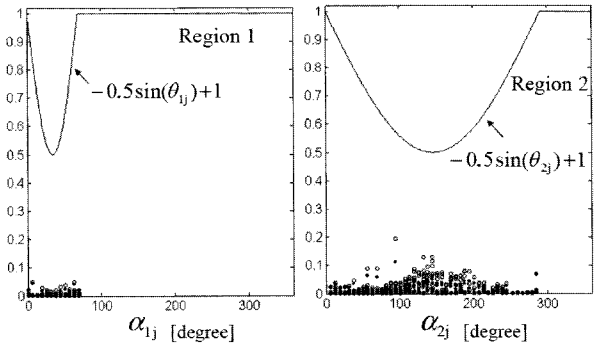

(b) Left turn.

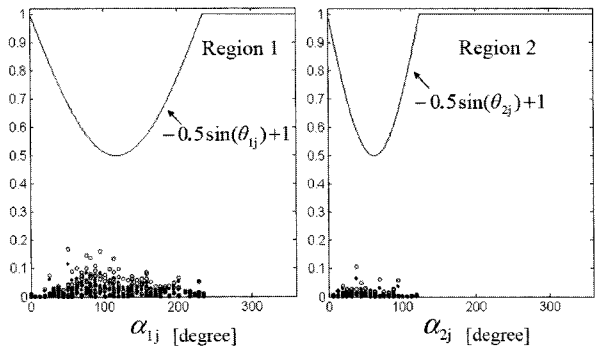

(c) Right turn.

Fig. 12. Characteristic of evaluation value $E_{t_{ij}}$ in straight forward, the left turn and right turn. 'o' describes $\frac{L_{\vec{v}_{ij}}}{\|\mathbf{L}_{\vec{v}}\|}\frac{L_{\vec{v}_{x_{ij}}}}{\|\mathbf{L}_{\vec{v}_x}\|}$, ' – ' presents $-0.5sin(\theta_{ij}) + 1$ and '•' shows $E_{t_{ij}}$.

mobile robot including straight forward, left turn and right turn. Specially, $L_{\vec{v}_{ij}} L_{\vec{v}_{x_{ij}}} / \|\mathbf{L}_{\vec{v}}\| \|\mathbf{L}_{\vec{v}_x}\|$, $-0.5 sin(\theta_{ij})$ and $E_{t_{ij}}$ are investigated in according to α_1 and α_2 in region 1 and 2, respectively. We can confirm that the calculated $E_{t_{ij}}$ becomes nearly uniform.

In case of rotation, let optical flow vector be $\vec{v}_i$, for $i = 1,...,L$ which L is the the number of optical flows. The evaluation value E_{r_i} is defined as follows:

$$E_{r_i} = \frac{L_{\vec{v}_i}}{\|\mathbf{L}_{\vec{v}}\|} \left(\left| \frac{1}{2} sin\left(\frac{\theta_i}{2} \right) \right| + \frac{1}{2} \right), \tag{13}$$

where $L_{\vec{v}_i}$ is the length of $\vec{v}_i$, $\mathbf{L}_{\vec{v}} = [L_{\vec{v}_1}, L_{\vec{v}_2}, ..., L_{\vec{v}_L}]$, and $\|\mathbf{L}_{\vec{v}}\|$ is the norm of $\mathbf{L}_{\vec{v}}$ and θ_i is the angle of optical flow vector from horizontal line as θ_{1j} and θ_{2j} are shown in Fig. 11. Because the optical flow is simple as shown in Figs. 4(b) and 6(b), the size and direction of optical flows are utilized. After all, if the calculated parameters $E_{t_{ij}}$ and E_{r_i} are larger than given values, their optical flows turn out to be the those of moving objects.

Fig. 13 shows the picture of the algorithm flowchart for detecting moving objects corresponding to Fig. 7.

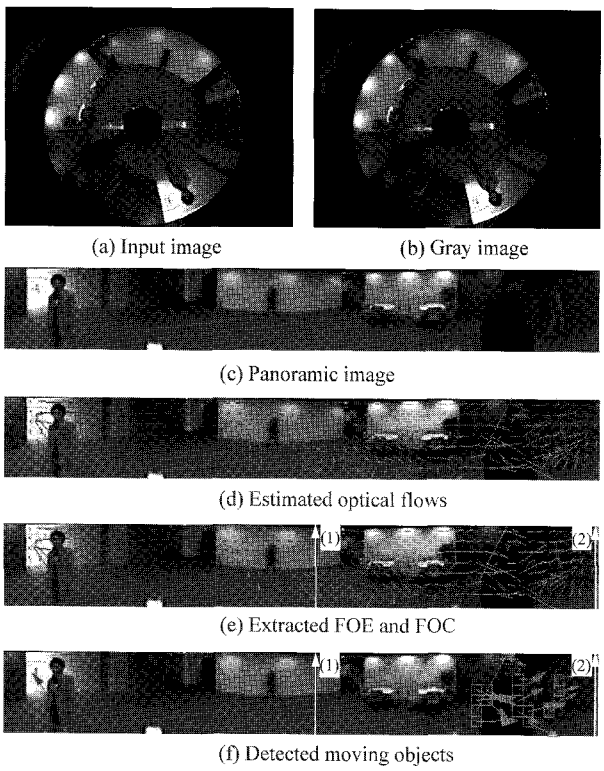

Fig. 13. Picture of the algorithm flowchart.

5. EXPERIMENT AND DISCUSSION

The omnidirectional camera is mounted on top of a mobile wheelchair robot moving in indoor environment. The proposed moving object detection method was applied to four motions mode including straight forward, left turn, right turn and rotation. The captured omnidirectional image size is 320×240 pixels. The expanded panoramic image size is 630×87 pixels. The frame rate of input image is 15 fps (frames per second). The color of input image is 24 bit RGB color. An optical flow was computed using a spatial local optimization [28]. The sample frames of detected moving objects in four motions are shown in Fig. 14. It is difficult to evaluate reasonably the proposed method in the dynamic motion of a mobile robot. The number of whole detected optical flow regions have been influenced on not only the size of spatial local region used for calculating optical flow but also the number and velocity of moving objects and distance between mobile robot and moving objects.

In this paper, in order to evaluate the proposed method, the error percentage is defined as the ratio of true optical flow among the detected optical flow of moving object. The error percentage of four motions are listed in Table 2. The frame number in straight forward, left turn, right turn, rotation is 71, 79, 72 and 78 frames, respectively. Error percentages of all motion are smaller than 4%. Fig. 15 describes the false detected optical flow region of moving objects among whole detected optical flow regions according to a series of frame in four motions.

Major reasons of wrong moving objects detection are the vibration of a mobile robot and the brightness variation in experiment environment. These vibration and brightness variation affects the estimation of

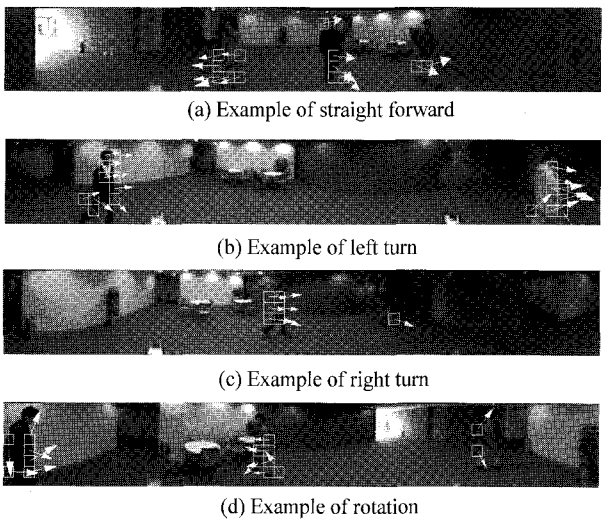

Fig. 14. Sample frames of detected moving objects in four motions.

Table 2. Error rate in four motions.

	Motion	Error rate[%]	# Frames
Movie 1	Straight	2.86	71
Movie 2	Left turn	3.80	79
Movie 3	Right turn	3.86	72
Movie 4	Rotation	2.15	78

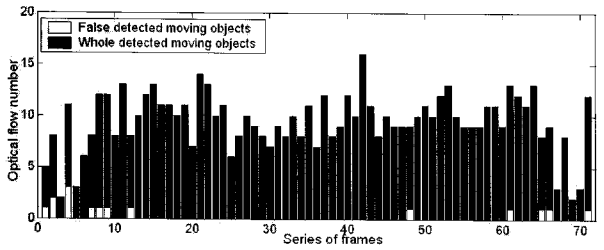

(a) Straight forward.

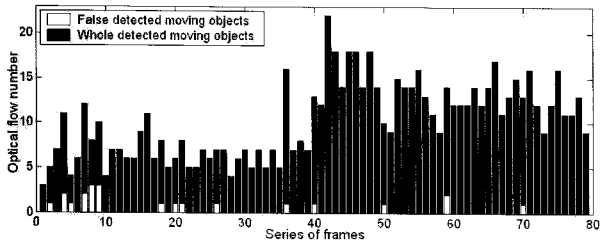

(b) Left turn.

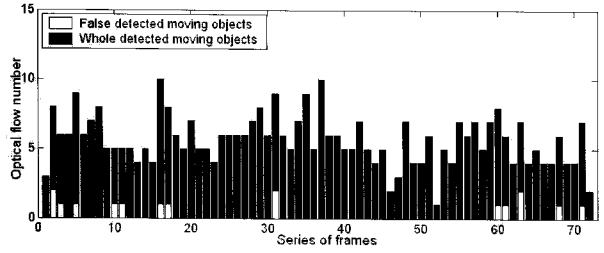

(c) Right turn.

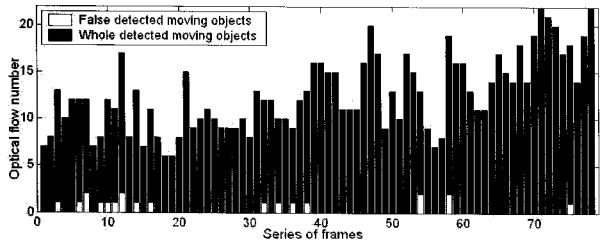

(d) Rotation.

Fig. 15. Optical flow number of detected moving objects in four motions.

optical flow. The wrong estimated optical flow cause the false detection of FOE and FOC vectors. In consequence, the false FOE and FOC vectors are not useful as reference vectors for detecting moving objects. The shadow of object also occurred the detection failure. Although the proposed method had some error, it described the robustness among the consecutive frame of four motions as shown in Fig. 15.

6. CONCLUSIONS

This paper presented a new moving object detection method in mobile robot with an omnidirectional camera. The optical flow was estimated using the spatial local optimization method for fast processing time. The optical flow which has been affected by the geometry characteristic of a hyperbolic mirror was investigated in omnidirectional and panoramic images. In case of translation of a mobile robot, FOE and FOC vectors were derived from the estimated optical flow were. FOE and FOC vectors were used as reference vectors to detect moving objects. In case of rotation of a mobile robot, the size and direction of optical flows were only used to detect moving objects. The moving obstacle was detected through the relative evaluation of optical flows. Especially, the filtering was suggested to eliminate the noise sensitivity of optical flow. Results of experiments using real moving images showed the effectiveness of the proposed method for detecting moving objects in mobile robot. As future work, it is necessary to reduce the vibration of mobile robot. Particularly, if we use (14), FOE and FOC vectors can be extracted from linear velocities V_x and V_y of the mobile robot which can be calculated by the motor encoder.

REFERENCES

[1] K. Yamazawa, Y. Yagi, and M. Yachida, "Omnidirectional imaging with hyperboloidal projection," *Proc. of IEEE Int. Conf. on Intelligent Robots and Systems*, vol. 2, pp. 1029-1034, July 1993.

[2] Y. Yagi, "Omnidirectional sensing and its application," *IEICE Trans. Information and Systems*, vol. E82-D, no. 3, pp. 568-579, 1999.

[3] J. Wolf, W. Burgard, and H. Burkhardt, "Robust vision-based localization by combining an image-retrieval system with Monte Carlo localization," *IEEE Trans. on Robotcis*, vol. 21, no. 2, pp. 208-216, 2005.

[4] S. Baker and S. Nayar, "A theory of single-viewpoint cata-viewpoint datadioptric image formation," *International Journal of Computer Vision*, vol. 35, no. 2, pp. 1-22, 1999.

[5] K. Daniilidis and C. Geyer, "Omnidirectional vision: Theory and algorithms," *Proc. of Int. Conf. on Pattern Recognition*, vol. 1, pp. 89-96, September 2000.

[6] J. Gluckman and S. K. Nayer, "Ego-motion and omnidirectional camera," *Proc. of Int. Conf. Computer Vision*, pp. 999-1005, January 1998.

[7] O. Shakernia, R. Vidal, and S. Sastry, "Infinitesimal motion estimation from multiple central panoramic views," *Proc. of IEEE Workshop on Motion and Video Computing*, pp. 229-234, December 2002.

[8] R. Vassallo, J. Santos-Victor, and J. Schneebeli, "A general approach for egomotion estimation with omnidirectional images," *Proc. of IEEE Workshop on Omnidirectional Vision*, pp. 97-103, June 2002.

[9] J. W. Lee, S. You, and U. Neumann, "Large motion estimation for omnidirectional vision," *Proc. IEEE Workshop on Omnidirectional Vision*, pp. 161-168, June 2000.

[10] J. Kim, M. Muramatsu, U. Murata, and Y. Suga, "Omnidirectional vision-based ego-pose estimation for an autonomus in-pipe mobile robot," *Advanced Robotics*, vol. 21. no. 3-4, pp. 441-460, 2007.

[11] T. Gandhi and M. Trivedi, "Motion based vehicle surround analysis using an omni-directional camera," *Proc. of IEEE Intelligent Vehicles Symposium*, pp. 560-565, June 2004.

[12] R. Runschotem and B. Krose, "Robust scene reconstruction from an omnidirectional vision system," *IEEE Trans. on Robotics and Automation*, vol. 19, no. 2, pp. 351-357, 2003.

[13] C. Drocourt, L. Delahoche, C. Pegard, and A. Clerentin, "Mobile robot localization based on an omnidirectional stereoscopic vision perception system," *Proc. of Int. Conf. on Robotics and Automation*, pp. 1329-1334, May 1999.

[14] E. Menegatti, A. Pretto, and E. Pagello, "A new omnidirectional vision sensor for Monte-Carlo localization," *Proc. of Int. RoboCup Symposium, LNAI*, vol. 3276, pp. 97-109, 2005.

[15] H. Koyasu, J. Miura, and Y. Shirai, "Mobile robot navigation in dynamic environments using omnidirectional stereo," *Proc. of Int. Conf. on Robotics and Automation*, vol. 1, pp. 893-898, Sep., 2003.

[16] Y. Yagi, K. Imai, K. Tsuji, and M. Yachida, "Iconic memory-based omnidirectional route panorama navigation," *IEEE Trans. on Pattern Analsis and Machine Intelligence*, vol. 27. no. 1, pp. 78-87, 2005.

[17] N. Winters, J. Gaspar, G. Lacey, and J. Santos-Victor, "Omni-directional vision for robot navigation," *Proc. of IEEE Workshop on Omnidirectional Vision*, pp. 21-28, June 2000.

[18] R. Nelson and Y. Aloimonous, "Obstacle avoidance using flow field eivergence," *IEEE Trans. on Pattern Analsis and Machine Intelligence*, vol. 11, no. 10, pp. 1102-1106, 1989.

[19] R. Sharma and J. Aloimonos, "Early detection of independent motion from active control of normal image flow pattern," *IEEE Trans. on Systems, Man, and Cybanetics*, vol. 26, no. 1, pp. 42-52, 1996.

[20] S. Fejes and L. S. Davis, "What can projections of flow fields tell us about the visual motion," *Proc. of Int. Conf. Computer Vision*, pp. 979-986, 1998.

[21] M. I. A. Lourakis, A. A. Argyros, and S. C. Orphanoudakis, "Independent 3D motion detection using residual parallax normal flow fields," *Proc. of Int. Conf. Computer Vision*, pp. 1012-1017, 1998.

[22] M. Watanabae, N. Takeda, and K. Onoguchi, "Moving obstacle detection and recognition by optical flow pattern analysis for mobile robots," *Advanced Robotics*, vol. 12, no. 8, pp. 791-816, 1999.

[23] H. S. Sawhney and Y. G. R. Kumar, "Independent motion detection in 3D scene," *Proc. of Int. Conf. Computer Vision*, pp. 612-619, 1999.

[24] Z. Hu and K. Uchimura, "Motion detection from a moving observer using pure feature matching," *Int. Jour. Robotics and Automation*, vol. 15, no. 1, pp. 21-26, 2000.

[25] A. Talukder, S. Goldberg, L. Matthies, and A. Ansar, "Real-time detection of moving objects in a dynamic sene from moving robotic vehicles," *Proc. of Int. Conf. Intelligent Robotics and systems*, pp. 1308-1313, 2003.

[26] I. Stratmann and E. Solda, "Omnidirectional vision and inertial clues for robot navigation," *Journal of Robotic Systems*, vol. 21, no. 1, pp. 33-39, 2004.

[27] K. Yamazawa, Y. Yagi, and M. Yachida, "Obstacle detection with omnidirectional image sensor hyperomni vision," *Proc. of International Conference on Robotics and Automation*, pp. 1062-1067, 1995.

[28] B. D. Lucas and T. Kanade, "An iterative image registration technique with an application to stereo vision," *Proc. of the 7th International Joint Conference on Artificial Intelligence*, pp. 674-679, April 1981.

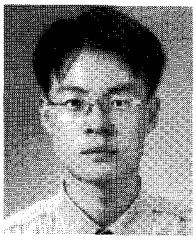

Jongcheol Kim received the B.E. degree in Control and Instrumentation Engineering from Changwon National University, Changwon, Korea, in 2000, and the M.S. degree in Electronic and Electrical Engineering from Pohang University of Science and Technology (POSTECH), Pohang, Korea, in 2002. He received the Ph.D. degree in Integrated Design Engineering at Keio University, Yokohama, Japan, in 2007. He is currently a Senior Researcher in Robot Business Department, KT. He was awarded the Best Paper Award from SCIS&ISIS2004, in 2004, and the Hujihara Award from Keio University, in 2005. His research interests include ubiquitous robot, HRI, computer vision, intelligent robot system and intelligent control.

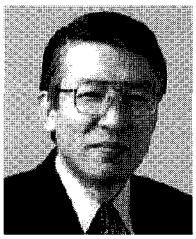

Yasuo Suga received the B.E., M.E. and Ph.D. degrees in Mechanical Engineering in 1970, 1972, and 1977, respectively, from Keio University. He is currently a Professor in Department of Mechanical Engineering at Keio University. His current research interest is machine vision, intelligent control system for industrial robots. He is a Member of JSME, JSPE, IEICE, JWS, ISOPE and so on. He was a Visiting Researcher at the Technische Hochschule Aachen (Germany), for 1982-83. From 1993 to 1994, he was the President of Materials and Processing Division of JSME. Currently he is a Director of Technical Commission on Joining and Materials Processing for Light Structures in JWS and the General Chair of International Symposium on Joining Technologies in Advanced Automobile Assembly 2005. He received the Materials and Processing Award from JSME in 1995 and Best Paper Award from SCIS&ISIS2004 in 2004.